Compression Waveforms for Non-Coherent Radar

Uri Peer and Nadav Levanon
Tel Aviv University
P. O. Box 39040, Tel Aviv, 69978 Israel
nadav@eng.tau.ac.il

Abstract - **Non-coherent pulse compression (NCPC) was suggested recently [1]. It was described using on-off keying (OOK) signals based on Manchester-coded binary pulse compression sequences (e.g., Barker, Ipatov). The present paper expands the discussion on waveform choice for both periodic and a-periodic cases, and on detection performances of this method. OOK transmitter and a receiver based on envelope-detection, suggested for the NCPC system, are simpler to implement than a binary phase-coded transmitter and a coherent receiver with I&Q synchronous detector, required for coherent pulse compression. NCPC can be used in simple radar systems where Doppler information is not required, in direct-detection laser radar systems and in ultra wide band (UWB) radar. Non-coherent processing has drawbacks in cases of reflections from multi-scatterer targets. The drawbacks and means of mitigating them are considered in section II.**

I. SCHEMATICS AND WAVEFORMS

We shall examine the receiving scheme shown in Fig. 1. This schematic performs correlation processing by utilizing a finite impulse response (FIR) filter, shown in the figure as a vector of constants (b_i, i = 1….n) which multiply the history of the received signal, after envelope detection (square-law, p=2, or linear-law, p=1) . In order to achieve high range resolution with low sidelobes, as well as good detection performances, there should be some complementary relationship between the transmitted signal and the coefficients of the FIR stored in the receiver. Noting the transmitted vector as $\boldsymbol{a}$ and the FIR filter (of the same length) as $\boldsymbol{b}$, without loss of generality we can first impose a normalization requirement,

$$\sum_{k=1}^{n} |a_k|^p b_k = 1 \tag{1}$$

where a_k and b_k are the elements of $\boldsymbol{a}$ and $\boldsymbol{b}$ respectively. In order to maintain low noise average at the output of the receiver, the FIR should be a band-pass filter (BPF) namely

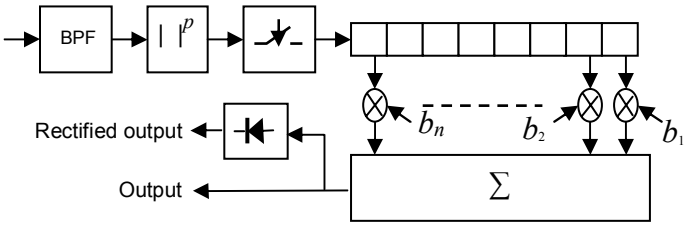

Fig. 1. Receiver block diagram

$$\bar{\boldsymbol{b}} = \frac{1}{n}\sum_{k=1}^{n} b_k = 0 \tag{2}$$

Two simple examples of NCPC signals are shown in Fig. 2 (a-periodic signal) and Fig. 6 (periodic signal). In the first example (Fig. 2), the transmitted signal (black) is based on the transmitted sequence $\boldsymbol{a}$, of length n=56, which is a Manchester-coded $(1 \to 10, 0 \to 01)$ MPSL 28 sequence [2, Table 6.3]:

$$\boldsymbol{a} = \{1\,0\,0\,1\,0\,1\,0\,1\,1\,0\,1\,0\,1\,0\,1\,0\,0\,1\,0\,1\,0\,1\,1\,0\,0\,1\,0\,1 \\ 0\,1\,1\,0\,0\,1\,0\,1\,0\,1\,1\,0\,0\,1\,0\,1\,1\,0\,0\,1\,1\,0\,1\,0\,0\,1\,1\,0\} \tag{3}$$

"1" in the transmitted sequence $\boldsymbol{a}$ is represented by a transmitted pulse in the corresponding time slot, while "0" is represented by a missing pulse. In the receiver the reflected pulses are envelope detected and cross-correlated, using the FIR filter, with a reference waveform (red) which is based on a reference complementary sequence $\boldsymbol{b}$, where:

$$\tilde{\boldsymbol{b}} = m\boldsymbol{b} = 28\boldsymbol{b} = 2\boldsymbol{a} - 1 = \{1\text{-}1\text{-}11\text{-}11\text{-}111\text{-}11\text{-}11\text{-}11\text{-}1\text{-}11\text{-}11\text{-}1 \\ 11\text{-}1\text{-}11\text{-}11\text{-}111\text{-}1\text{-}11\text{-}11\text{-}111\text{-}1\text{-}11\text{-}111\text{-}1\text{-}111\text{-}11\text{-}1\text{-}111\text{-}1\} \tag{4}$$

m is the number of '1's in the transmitted sequence $\boldsymbol{a}$ and $\tilde{\boldsymbol{b}}$ is the unnormalized $\boldsymbol{b}$. In other words the reference signal differs from the transmitted signal by inserting negative pulses at the locations corresponding to "0" in the transmitted sequence.

The lower subplot of Fig. 2 shows the outcome of the cross-correlation between the two signals $\boldsymbol{a}$ and $\boldsymbol{b}$. It maintains the general low peak sidelobe ratio $(2/28)$ found in the autocorrelation of the original MPSL 28 signal, except for the two negative near sidelobes, whose sum is almost equal to the height of the mainlobe. Note that the mainlobe width depends on the width of the pulses (transmitted and reference) rather than on the duration of a sequence element. Narrowing the pulses will narrow the mainlobe width, but will require wider bandwidth, hence more noise at the input to the envelope detector. In Fig 2 the cross-correlation vector $\boldsymbol{c}$ was multiplied by m (=28), for presentation purposes only.

For Manchester-coded binary sequences the reference vector $\boldsymbol{b}$ contains a small set of values (in our example: 1/28,-1/28), which further simplifies the receiver. In a-periodic cases filter $\boldsymbol{b}$ can be longer than signal $\boldsymbol{a}$. In that case the normalization in (1) will be replaced by the requirement that the cross-correlation vector $\boldsymbol{c}$ will get a value of '1' at zero delay.

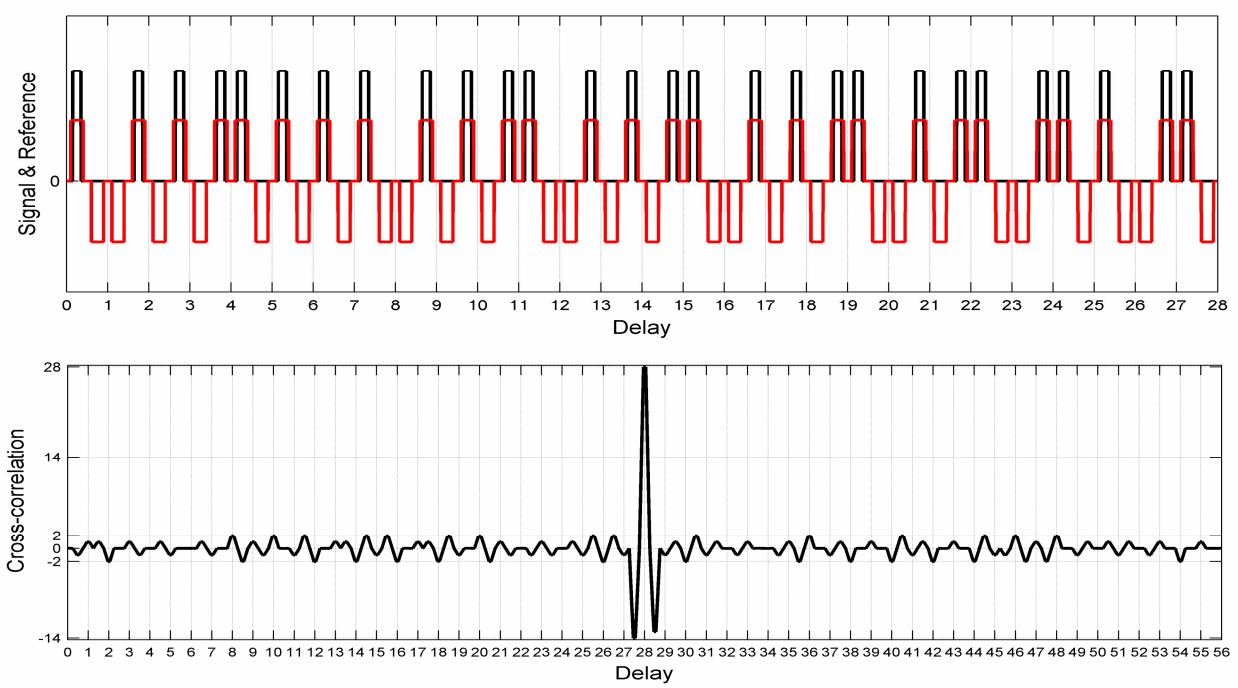

Fig.2. Top: Transmitted (black) and reference (red) signals, based on Manchester-coded MPSL 28. Bottom: Cross-correlation between the transmitted and reference signals.

II. Sensitivity of NCPC to Multiple-Scatterers

Before proceeding to the periodic signal example, we pause to discuss a major difficulty that may hamper non-linear detection. It affects both periodic and a-periodic waveforms, but will be demonstrated using the a-periodic signal introduced in the previous section.

Coherent receiver, matched or mismatched, processing a reflected coherent compressed pulse, is only slightly affected by the presence of two or more scatterers. Consider coherent transmission of the OOK signal whose complex envelope was represented by the sequence $\boldsymbol{a}$ and a receiver that performs coherent synchronous detection of that complex envelope, and cross-correlate it with $\boldsymbol{b}$. Assume also that the received reflected signal results from two scatterers yielding the received, noise-free, complex envelope:

$$u(t) = u_1(t) + u_2(t) \tag{5}$$

$$u_1(t) = a(t) \tag{6}$$

$$u_2(t) = \alpha \exp(-j\beta) a(t-\tau) \tag{7}$$

where α is a real positive number that represents the relative intensity, β is the relative phase in radians and τ is the delay difference between the two reflections. The linear processing performed in the coherent receiver yields the output

$$v_L(t) = u(t) \otimes b(t) = a(t) \otimes b(t) + \alpha \exp(-j\beta) a(t-\tau) \otimes b(t) \tag{8}$$

where $\otimes$ represents cross-correlation.

If the cross-correlation between $\boldsymbol{a}$ and $\boldsymbol{b}$ exhibits low peak-sidelobes ratio (e.g., in the Manchester-coded MPSL-28 signal, PSLR=1/14), and if the delay difference τ is larger than one bit duration, then the magnitude of the output $|v_L(t)|$ will include the original two mainlobes, separated by τ, whose normalized peak values P_1 and P_2 would be bounded by

$$|1 - \alpha \mathrm{PSLR}| \le P_1 \le 1 + \alpha \mathrm{PSLR} \tag{9}$$

$$|\alpha - \mathrm{PSLR}| \le P_2 \le \alpha + \mathrm{PSLR} \tag{10}$$

In contrast, the non-coherent processor performs envelope detection prior to the cross-correlation operation. Assuming p=1 in Fig. 1, the output of the non-linear processor would be

$$v_{NL}(t) = |u(t)| \otimes b(t) = |a(t) + \alpha \exp(-j\beta) a(t-\tau)| \otimes b(t) \tag{11}$$

With this kind of processor the effect on the two mainlobes of the cross-correlation could be more drastic, and could not be bounded as in (9) and (10). A comparison between linear and non-linear processing is shown in Figs. 3 and 4. In that example $\tau = 8.25 t_b$ and $\alpha = 0.9$. The phase difference β is 3.5 radians (= 200^0). The pulse-width is half the bit duration.

The top subplot of Fig. 3 shows the first reflected signal. The second subplot shows the magnitude of the second signal, separated by 8.25 bits and slightly attenuated. The two signals add coherently at the antenna and the magnitude of their sum is shown in the third subplot of Fig. 3. We will come back to the bottom subplot shortly.

The top subplot of Fig. 4 shows the magnitude of the output of a synchronous coherent detector that performs what was described in equation (8).

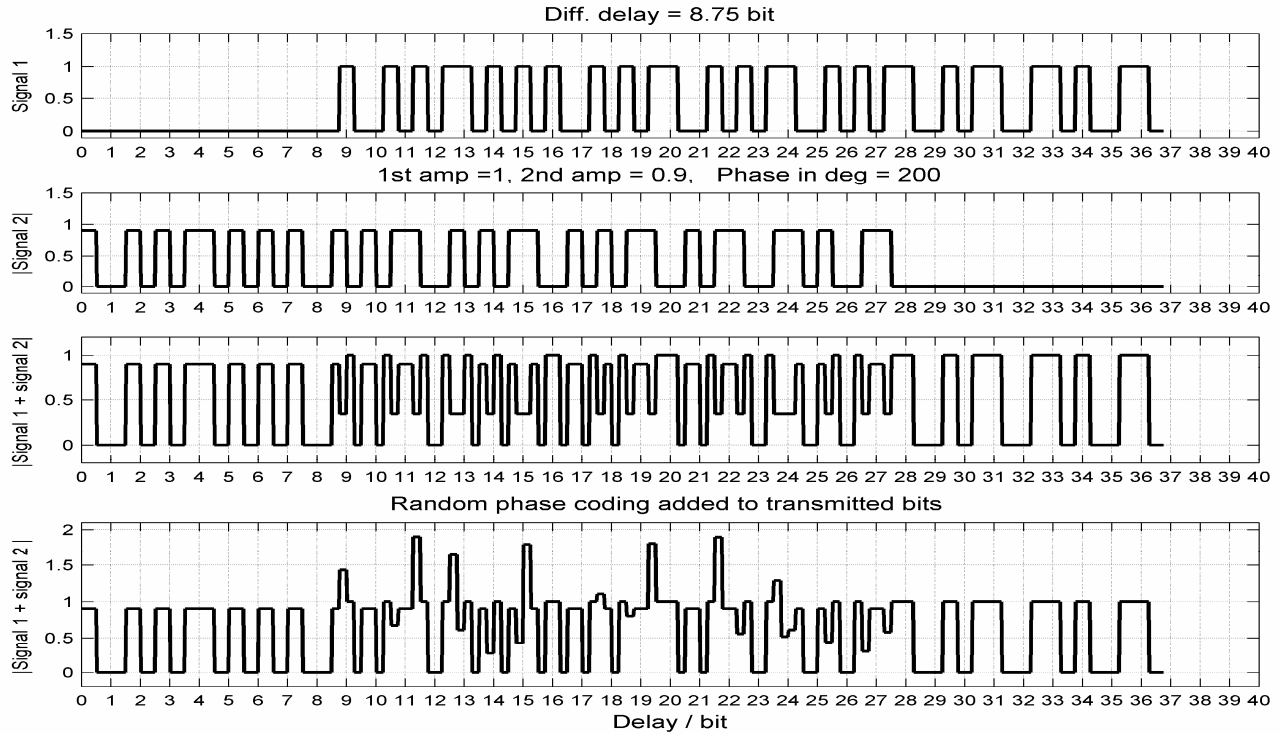

Fig. 3. Signals reflected from two scatterers

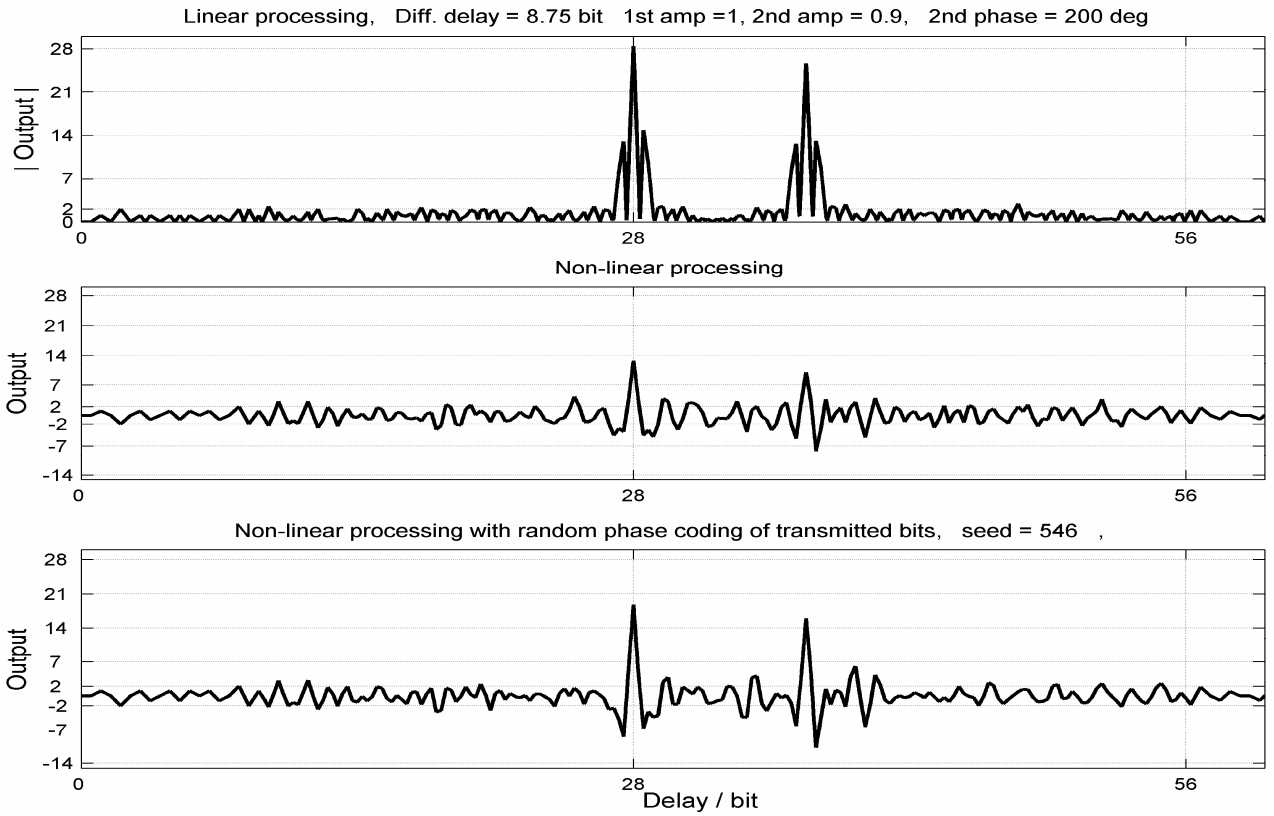

Fig. 4. Detection outputs of the signals in Fig. 3.

Note that each one of the two peaks is hardly affected by the presence of the other reflection, and maintains its relative strength (28.4 instead of 28 and 25.7 instead of 25.2) as predicted by (9) and (10). The second subplot of Fig. 4 shows the output of the non-linear detector that performs equation (11). Comparing it to the single scatterer case (bottom subplot of Fig. 2) we note considerable degradation of performances.

A possible remedy that can mitigate the degradation caused by multiple scatterers is to add random phase coding to the transmitted pulses (bits). As a matter of fact, such random interpulse phase modulation is inherent in some practical transmitters, e.g., lasers, magnetrons. Detection performances in a single scatterer scenario will not be affected by such phase modulation, because envelope detection is transparent to phase coding. However, reflections from two scatterers, spaced in delay by several bits, add coherently at the receiving antenna, and are likely to average out when a different and random phase modulates each bit. An example of the magnitude of the resulted signal is shown in the bottom subplot of Fig. 3 and the output of the non-linear detector is shown in the bottom subplot of Fig. 4. For that specific scenario, the improvement caused by the added random phase coding is rather prominent. In order to quantify the contribution of random phase coding on transmit, we performed a Monte-Carlo simulation, whose results are summarized in Fig. 5. In that simulated situation the relative intensity of the second reflection was 0.9. The phase coding was random from bit to bit and changed from run to run. 40000 runs were performed for each choice of spacing between the two reflections. They differed by the reflections phase difference β, drawn from a uniform probability density function (PDF). Random phase coding was added only in the "NCPC + rnd phase" case (solid, black). The thresholds were set so that each one of the two detectors (coherent and non-coherent) will yield the same probability of false alarm, $P_{FA} = 0.001$. The signal-to-noise ratios (SNR) were set to yield $P_D = 0.95$ in a single reflector case. Indeed that is the probability of detection observed in Fig. 5, for all three cases, when the spacing is larger than the signal length of 28 bits. The required SNR for non-coherent detection was 1.9dB larger than for the coherent detection. This SNR loss is due to the difference between coherent and non-coherent detectors. There is an additional loss caused by the mismatch. In a coherent system the original phase-coded MPSL signal could have been transmitted, for which a matched receiver yields good response.

Fig. 5 shows that for coherent detection (dotted, red), there is practically no degradation when the separation is longer than one bit. With non-coherent (envelope) detection, when no phase coding is added (dash, blue), the degradation in P_D increases as the separation decreases, reaching $P_D \approx 0.67$ for a separation of one bit. When random phase coding was added (solid, black) the probability of detection is up again, fluctuating between 0.85 and the desired P_D value of 0.95.

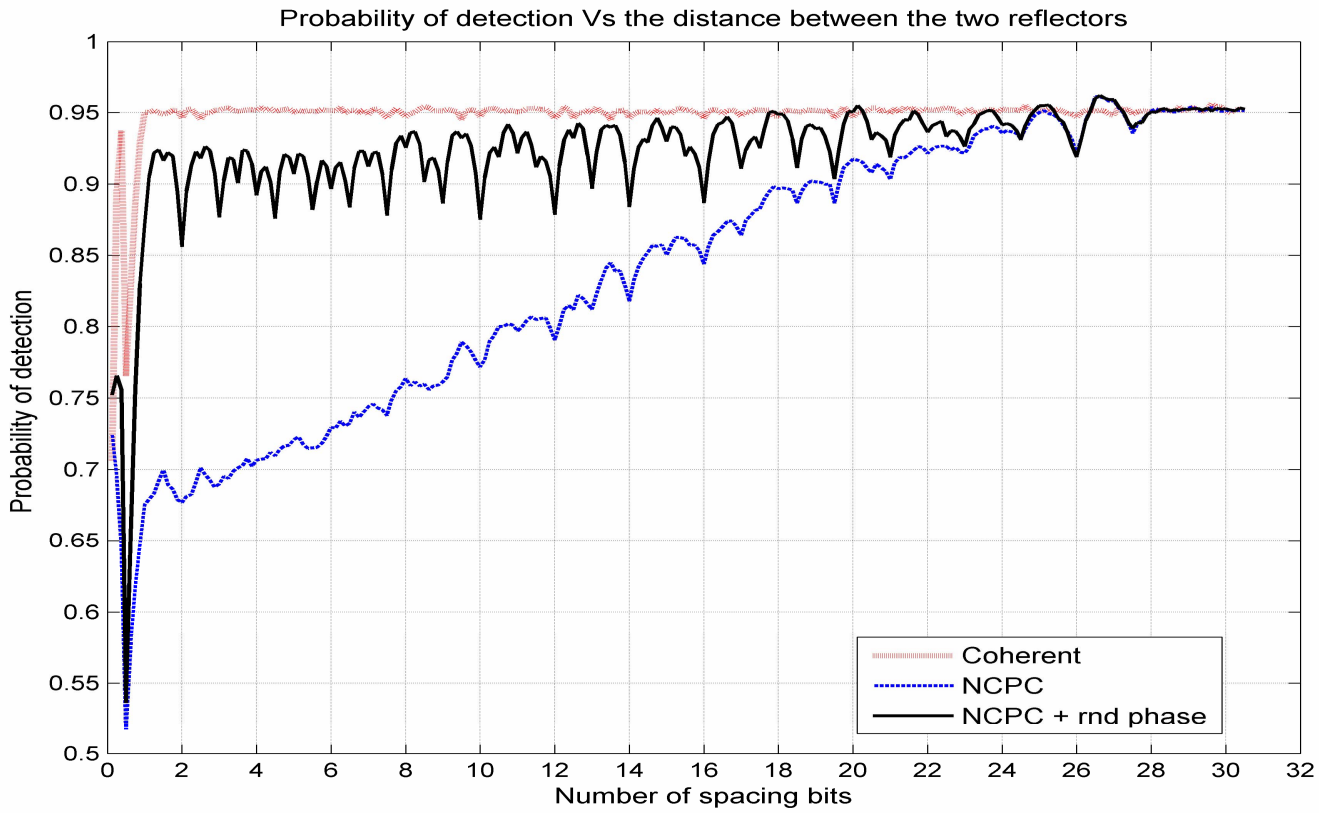

Fig. 5. Detection performances of coherent and non-coherent detection of Manchester-coded MPSL 28 signal, with and without random phase coding.

The conclusion is that adding random phase modulation to the transmitted pulses is advantageous for multi-scatterer or extended targets, but has no effect on detecting single-scatterer targets. As pointed out already, there are situations when the phase of the individual pulses is inherently changing randomly from pulse to pulse.

III. Periodic Waveform

For the second example (periodic signal) a 24 elements Ipatov code [3], [2 (Sec. 6.5)] was Manchester-coded to get a desired transmitted sequence $\boldsymbol{a}$. Then a reference sequence $\boldsymbol{b}$ was found in order to yield a specific cross-correlation.

$$\boldsymbol{a}=\{101010010101100101010101100101100110100101011001\} \quad (12)$$

$$\boldsymbol{b} = \{q\ -q\ r\ -r\ r\ -r\ -s\ s\ -s\ s\ -s\ s\ q\ -q\ -s\ s\ -s\ s\ -s\ s\ -s\ s\ -s\ s\ q\ -q\ -s\ s\ -s\ s\ r\ -r\ -s\ s\ r\ -r\ q\ -q\ -s\ s\ -s\ s\ -s\ s\ r\ -r\ -s\ s\} \quad (13)$$

where q =5/180, r = 11/180, s = 7/180.

The periodic signal, reference, and cross-correlation are shown in Fig.6. In the middle subplot the reference signal was multiplied by 180 for presentation purposes only. The lower subplot shows that the perfect cross-correlation found in the original Ipatov code is maintained, except for the two negative sidelobes.

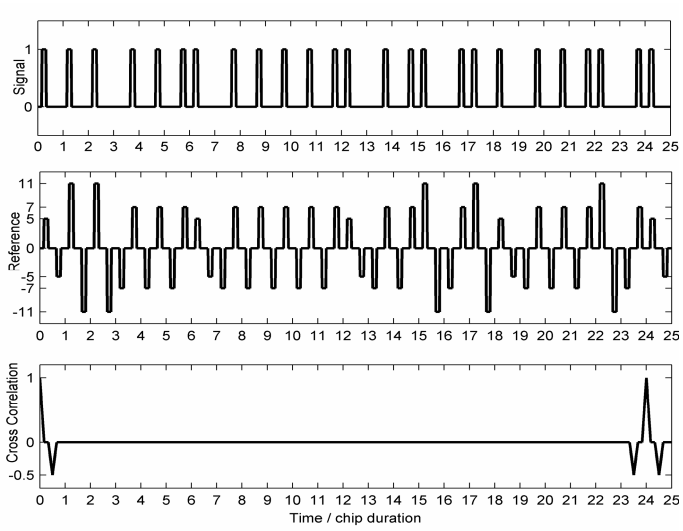

Fig.6. One period of Manchester-coded Ipatov 24: Signal, reference and cross-correlation.

IV. Finding Complementary Sequences

Manchester coding a known binary code is only one family of possible transmission sequences. Its advantage is maintaining the original code properties (i.e., low-sidelobe binary code will become low-sidelobe OOK sequence). In order to find the transmitted sequence $\boldsymbol{a}$ and the reference sequence $\boldsymbol{b}$ for the general case, we have defined performance functions both for the periodic and the a-periodic case. Once a performance function is defined, one searches for a sequence that will bring the performance to a maximum.

Of the many possible search algorithms we have adopted the Hill Climbing method to our application, and used it successfully to find the desired sequences. This method was used in [4] to find optimal sequences for mismatch filters. It is a special case of the simulated annealing search method.

For the periodic case, with a desired cross-correlation $\boldsymbol{c}$, transmitted sequence $\boldsymbol{a}$ and reference sequence $\boldsymbol{b}$, the performance function is as follows

$$f_{\text{periodic}}(\boldsymbol{a},\boldsymbol{c}) = \boldsymbol{c}\boldsymbol{A}\left(\boldsymbol{A}^{\mathsf{T}}\boldsymbol{A}\right)^{-1}\left[\left(\boldsymbol{A}^{\mathsf{T}}\boldsymbol{A}\right)^{-1}\right]^{\mathsf{T}}\boldsymbol{A}^{\mathsf{T}}\boldsymbol{c}^{\mathsf{T}} = \boldsymbol{b}\boldsymbol{b}^{\mathsf{T}} \quad (14)$$

where

$$\boldsymbol{A} = \begin{bmatrix} a_1^p & a_2^p & \cdots & a_n^p \\ a_n^p & a_1^p & \cdots & a_{n-1}^p \\ \vdots & \ddots & \ddots & \vdots \\ a_2^p & \cdots & a_n^p & a_1^p \end{bmatrix} \quad (15)$$

and

$$\boldsymbol{b} = \boldsymbol{c}\boldsymbol{A}\left(\boldsymbol{A}^{\mathsf{T}}\boldsymbol{A}\right)^{-1} \quad (16)$$

In the a-periodic case, $\boldsymbol{b}$ is the minimum ISL mismatched filter of length l for the sequence $\boldsymbol{a}$, and the performance function is

$$f_{\text{a-periodic}}(\boldsymbol{a},l) = \text{ISL level of the cross - correlation} \quad (17)$$

where the cross-correlation vector $\boldsymbol{c}$ will be normalized to yield '1' at zero delay, in order to satisfy (1). We found it advantageous to exclude the first near sidelobe (on both sides) from the ISL minimization. These two correlation sidelobes are inherently negative and will be removed by the one-way rectifier. Fig. 7 demonstrates the sidelobe reduction achieved by using a long (280 element) mismatched filter to the 56 element Manchester-coded MPSL 28. The peak sidelobe dropped from -22.9 dB to -41.3 dB. The added SNR loss (not shown) was 1.4 dB.

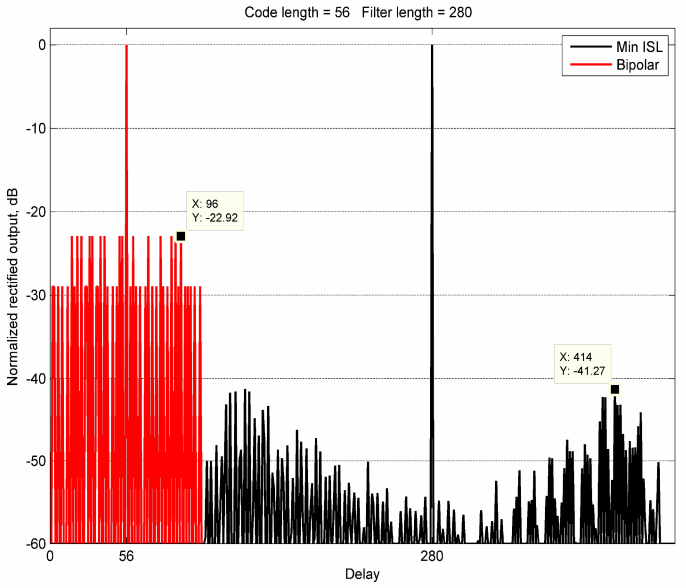

Fig.7. Normalized rectified output with 56 element bipolar (red) and 280 element minimum-ISL (black) filters

V. Detection Performances

The a-periodic example (Manchester-coded MPSL 28) will serve to quantify the detection properties, using theory and simulations. Detection performances, corresponding to the peak of the cross-correlation output, were calculated assuming square-law envelope detection, a non-fluctuating, single scatterer target, and additive white Gaussian noise (AWGN). Let the received signal be a row complex vector,

$$r_k = A_0 a_k + v_k + j u_k \quad , \quad k = 1,2,.....n \ , \ v_k \in \mathrm{N}(0,\sigma) \ , \ u_k \in \mathrm{N}(0,\sigma) \tag{18}$$

where A_0 is the non-fluctuating amplitude of the reflected pulses, v and u are the in-phase and quadrature-phase components of the noise, and all three defined at the output of the BPF. Both v and u are taken from zero-mean Gaussian probability density function (PDF), with standard deviation σ (a function of the BPF bandwidth). The input single-pulse signal-to-noise ratio (*SNR*) is define as

$$SNR = \frac{A_0^2}{2\sigma^2} \tag{19}$$

The output of the square-law envelope detector is obtained from (18)

$$s_k = \left(A_0 a_k + v_k\right)^2 + u_k^2 \quad , \quad k = 1,2,.....,n \tag{20}$$

and the peak of the cross-correlation will be

$$x = \boldsymbol{s} * \boldsymbol{b}^{\mathsf{T}} \tag{21}$$

where $(\,)^{\mathsf{T}}$ is the transpose operation.

An approximate PDF of x can be calculated using the central limit theorem. We will get a Gaussian PDF

$$p(x) \approx \mathrm{N}(\mu_x, \sigma_x) \tag{22}$$

$$\mu_x = A_0^2 \tag{23}$$

where (23) holds because of properties (1) and (2), and

$$\begin{aligned} &\mathrm{var}(x) = \sigma_x^2 = \boldsymbol{b}\boldsymbol{W}_0\boldsymbol{b}^{\mathsf{T}} \\ &\text{where } \boldsymbol{W}_0 = \mathrm{diag}\left(\left[8\sigma^4\left(0.5 + a_1^2\, SNR\right), \cdots, 8\sigma^4\left(0.5 + a_n^2\, SNR\right)\right]\right) \end{aligned} \tag{24}$$

Without target (noise only), x is still a normally distributed r.v.

$$p\left(x \middle| A_0 = 0\right) \approx \mathrm{N}\left(\mu_{x|A_0=0}, \sigma_{x|A_0=0}\right) \tag{25}$$

$$\mu_{x|A_0=0} = 0 \tag{26}$$

$$\mathrm{var}\left(x \middle| A_0 = 0\right) = 4\sigma^4 \boldsymbol{b}\boldsymbol{b}^{\mathsf{T}} \tag{27}$$

In the special case in which the reference is composed out of two value set {1/m, -1/m} and the transmitted sequence is composed out of {1,0}, equation (24) takes the following form:

$$\mathrm{var}(x) = \sigma_x^2 = \frac{4\sigma^2}{m^2}\left(n\sigma^2 + mA_0^2\right) = \frac{8\sigma^4}{m^2}\left(\frac{n}{2} + mSNR\right) \tag{28}$$

Furthermore, if $n = 2m$, as in a Manchester-coded sequence, (28) will become

$$\mathrm{var}(x) = \sigma_x^2 \underset{n=2m}{=} \frac{8\sigma^4}{m}\left(1 + SNR\right) \tag{29}$$

The PDFs in (22) to (29) were also numerically calculated for the first example (Manchester-coded MPSL 28 sequence) using Monte-Carlo simulations. Both numerical and theoretical results are plotted on top of each other in Fig. 8. Note that the PDFs derived from theory and from the histogram agree very well in the noise-only case and to a lesser degree when signal is present.

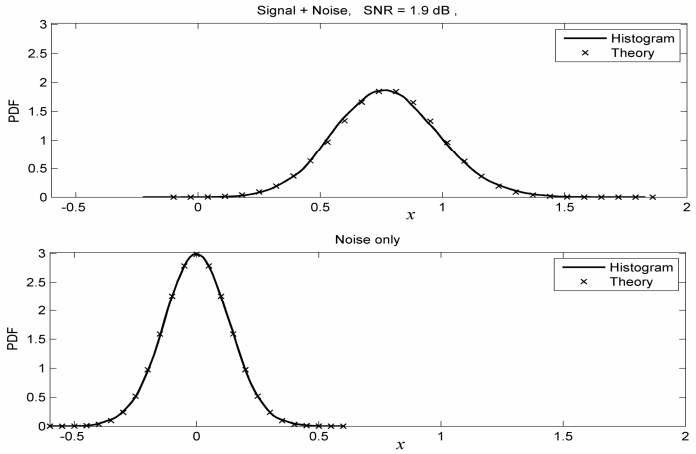

Fig. 8. PDFs corresponding to non-coherent pulse compression. Top: signal + noise, Bottom: noise only

The histograms of x and x_{noise} were obtained with 40000 Monte-Carlo runs. The histograms were created using $\sigma = 0.5$. To get the desired probability of false alarm $\left(P_{\text{FA}} = 0.001\right)$ the threshold was set at 0.43. To get the desired probability of detection $\left(P_{\text{D}} = 0.95\right)$ required single-pulse *SNR* of 1.9dB.

Similar analysis can be performed in the periodic case. There however it is possible to integrate (non-coherently) many periods, and achieve further SNR gain.

Acknowledgment

Section II was prompted by very helpful comments from J. Mike Baden and Marvin N. Cohen, based on their field results with the ill-fated Intrapulse Polarization Agile Radar (IPAR) [5]. We are indebted to Mike Baden for many ensuing discussions and suggestions.

References

[1] N. Levanon, "Noncoherent pulse compression,". *IEEE Transactions on Aerospace and Electronic Systems*, vol. 42, pp. 756-765, April 2006.

[2] N. Levanon, and E. Mozeson, *Radar Signals.* New York, NY: Wiley, 2004.

[3] V. P. Ipatov, and B. V. Fedorov, "Regular binary sequences with small losses in suppressing sidelobes," *Radioelectron. a. Commun. Syst. (Radioelektronica)*, vol. 27, no. 3, pp. 29-33, 1984.

[4] K. R. Griep, J. A. Ritcey, and J. J. Burlingame, "Poly-phase codes and optimal filters for multiple user ranging," *IEEE Transactions on Aerospace and Electronic Systems*, vol. 31, pp. 752-767, April 1995.

[5] M. N. Cohen, B. Perry, and J. M. Baden, "Preliminary analysis of IPAR performances," *Proceedings of the 1984 IEEE National Radar Conference*, 1984, pp. 37-42.